IONIC PERMEABILITY OF K, Na, AND Cl IN CRAYFISH NERVE

REGULATION BY MEMBRANE FIXED CHARGES AND pH

ALFRED STRICKHOLM AND HULDA R. CLARK, *Section of Physiology, Medical Sciences Program, Indiana University, Bloomington, Indiana 47401 U.S.A.*

ABSTRACT Teorell's fixed charge theory for membrane ion permeability was utilized to calculate specific ionic permeabilities from measurements of membrane potential, conductance, and specific ionic transference numbers. The results were compared with the passive ionic conductances calculated from the branched equivalent circuit membrane model of Hodgkin and Huxley. Ionic permeabilities for potassium, sodium, and chloride of crayfish (*Procambarus clarkii*) medial giant axons were examined over an external pH range from 3.8 to 11.4. Action potentials were obtained over this pH range. Failures occurred below pH 3.8 during protonation of membrane phospholipid phosphate and carboxyl, and above pH 11.4 from calcium precipitation. In general, chloride permeability increases with membrane protonation, while cation permeability decreases. At pH 7.0, $P_K = 1.33 \times 10^{-5}$, $P_{Cl} = 1.49 \times 10^{-6}$, $P_{Na} = 1.92 \times 10^{-8}$ cm/s. $P_K : P_{Cl} : P_{Na} = 693:78:1$. P_{Cl} is zero above pH 10.6 and is opened predominately by protonation of ϵ-amino, and partially by tyrosine and sulfhydryl groups from pH 10.6 to 9. P_K is activated in part by ionization of phospholipid phosphate and carboxyl around pH 4, then further by imidazole from pH 5 to 7, and then predominately from pH 7 to 9 by most probably phosphatidic acid. P_{Na} permeability parallels that of potassium from pH 5 to 9.4. Below pH 5 and above pH 9.4, P_{Na} increases while P_K decreases. Evidence was obtained that these ions possibly share common passive permeable channels. The data best support the theory of Teorell, that membrane fixed charges regulate ionic permeability and that essentially every membrane ionizable group appears involved in various amounts in ionic permeability control.

INTRODUCTION

An important problem in membrane physiology is the molecular mechanism by which ionic permeability is regulated. Important contributions to this problem have come from studies utilizing artificial bimolecular lipid membranes (BLM) separating two liquid phases. These studies show that a lipid bilayer membrane ordinarily has very low ionic permeability, typically one millionth that of natural membranes. It is only when other components, often proteinaceous, are added to the lipid bilayer that excitation and ionic permeabilities comparable to natural membranes are attainable (Mueller and Rudin, 1968; Tien, 1974; Jain, 1972). Thus the addition to a lipid bilayer of components, such as the sodium-potassium coupled ion transport system (Jain et al., 1972),

produces an increase in membrane ion permeability. This permeability increase could result from a permeable pathway or ion leak separate from the incorporated components primary function or activity. If the components incorporated in cell membranes responsible for ion permeation have titratable ionizable groups, a study of the pH dependency of ion permeation may provide information on the topology of these incorporated components in membranes and the mechanism of membrane ion transport. This paper describes experiments which delineate the dependency of potassium, sodium, and chloride permeability, and conductance on pH in resting nerve membrane. An earlier report on this had been made (Strickholm et al., 1969). Comparisons are made here between the fixed charge theory of Teorell (1953) for membrane permeability through a homogenous domain, and the conductance formulation of the parallel branched equivalent circuit (Hodgkin and Huxley, 1952; Schwartz, 1971).

METHODS

Giant axons, 50–200 μm in diameter, from the ventral nerve chord of the crayfish *Procambarus clarkii* were examined over several years in these studies. The external sheath was removed and one of the medial giant axons was isolated completely or partially (enough to permit rapid ion diffusional access) from other axons for a distance of more than six length constants (λ) and mounted in a chamber that allowed rapid exchange of the external solution (Fig. 1). Two holes were cut at opposing ends of the axon, through which a potential recording and a constant current-injecting microelectrode were axially inserted and advanced (to measure λ), until their tips were nearly adjacent, and the axon cable input impedance (Z_i) was measured. A small ball of insulating lacquer was placed just behind each microelectrode tip to minimize accidental injury to the axon surface during electrode advancement. A single accidental penetration of the axon surface always reduced input cable impedance irreversibly and invariably resulted in mem-

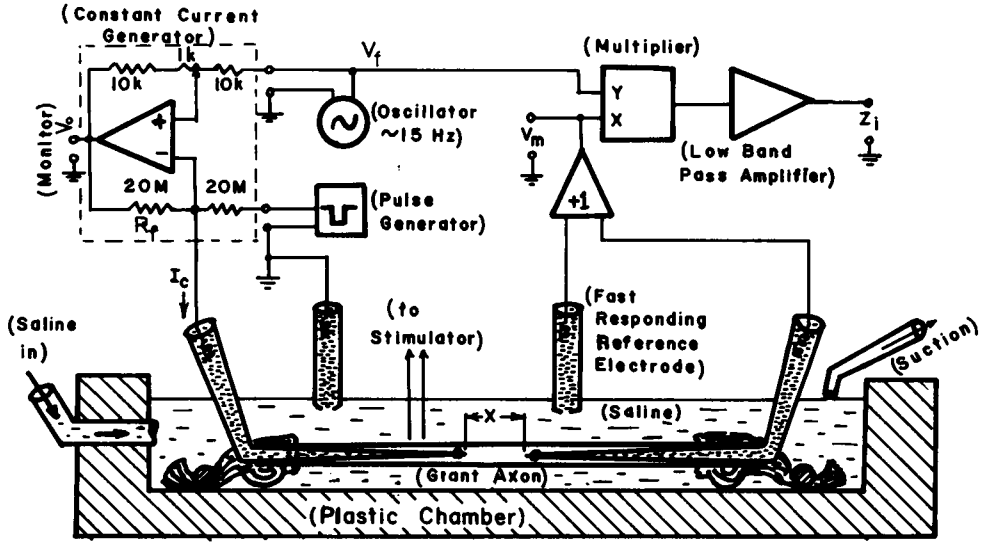

FIGURE 1 Method for measuring nerve cable properties and ionic permeability.

brane potential failure (typically 50 mV in 30 min). Only axons whose membranes had never been penetrated were included in these studies.

Membrane potential was recorded by a high input impedance capacitive-compensated headstage amplifier and displayed on an oscilloscope and one channel of an ink-writing pen recorder. The reference salt bridge electrode for potential measurement was of the fast response conical design that reduces the long-term (typically minutes to hours) potential transient errors of over 4 mV which occur during the saline changes here with cylindrical salt bridge reference electrodes (Strickholm, 1968; Strickholm and Wallin, 1967, p. 1949). An uncharged gel (Agarose, Bausch and Lomb, Rochester, New York) was used in the salt bridge to prevent liquid junction potential changes at different pH's, and to prevent bulk salt flow. Constant current was injected into the current electrode by the Howland (1966) circuit (see Fig. 1), which has an infinite output impedance and thus does not load the axon cable impedance or membrane potential. A field-effect transistor operational amplifier was used here. The output current of this circuit is V_{in}/R_f, where V_{in} is the voltage input to the constant current generator, and R_f the circuitry feedback resistor (2×10^7 Ω here). The constant current generator monitor output, V_0, was recorded to indicate membrane potential $V_m = V_0/2$ (with no current injection), and whether circuitry limiting occurs due to current saturation of the microelectrode. Into one input of the constant current generator, step voltage pulses (plus or minus) of several seconds duration were applied to determine the linearity of the current-voltage relation of the axon input impedance (see Fig. 2 *a*). Into the other input, a sinusoidal signal (ca. 1 V, 15 Hz) was applied to provide continuous measurement of the axon cable input impedance at zero membrane current. The sinusoidal current output was ordinarily 5×10^{-8} A, which produced typically 2–3 mV across the axon membrane at the current electrode tip. A sine wave frequency of 15 Hz was chosen because it permitted DC analysis of axon cable properties; it was attenuated sufficiently by the frequence response of the DC pen recorder (Omniscribe, Houston

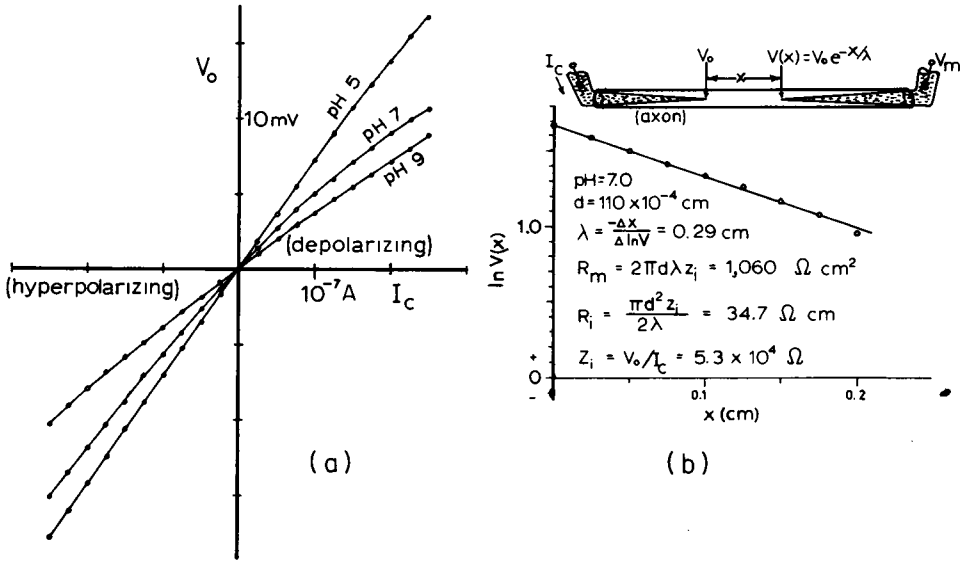

FIGURE 2 *a*. The relationship of membrane potential to input current across the axon cable input impedance. No rectification is observed at zero membrane current. *b*. Different axon from *a*. The membrane potential as a function of the distance *x* from the current electrode.

Instrument Div., Bausch & Lomb, Inc., Austin, Tex.) so as to not interfere with the membrane potential measurements; and in the cable impedance measuring circuitry, the half-time response to membrane resistive changes could be set to under 1 s.

The voltage and current-injecting electrodes were advanced toward each other and the potential $V(x)$ produced by current injection (by voltage pulses and sine wave) was recorded as a function of the distance, x, separating the two electrode tips (Figs. 1 and 2*b*). Both DC and 15 Hz measurements gave identical results. From ideal DC cable theory, $V(x) = V(x = 0) \exp(-x/\lambda)$. The length constant was determined as $\lambda = -\Delta x/\Delta \ln[V(x)]$ (see Fig. 2*b*). Ordinarily for $x = 0$, the electrode tips were kept around 20 μm apart to avoid the near field potential gradients at the current electrode tip. The contribution of this coupling resistance to the total cable input impedance was thus kept below 2% for a 1-μm tip diameter current-injecting electrode. When the two electrodes adjoin, $V(x = 0) = IZ_i$, where I is the injected current, and Z_i the input impedance of two axon cable impedances in parallel. If the distance from the electrode tips to their entry holes are several length constants, as is the situation here, the end voltage reflections can be ignored (see Weidman, 1952) and $Z_i = Z/2$, where Z is the infinite cable impedance. DC cable theory gives: $Z = [r_m(r_i + r_e)]^{1/2}$ and $\lambda = [r_m/(r_i + r_e)]^{1/2}$, where r_m is the membrane resistance per unit length of fiber and r_i and r_e are the axoplasmic and external resistances per unit length. For an axon of cross sectional area A and surface perimeter P, and neglecting r_e (ordinarily $r_e < r_i$), we have: $R_m = 2P\lambda Z_i$, and $R_i = 2AZ_i/\lambda$, where R_m (Ω cm^2) is the specific membrane resistance and R_i (Ω cm) the specific axoplasmic resistance. For a cylindrical axon of diameter d these become: $R_i = \pi d^2 Z_i/2\lambda$, and $R_m = 2\pi d\lambda Z_i = (\pi^2 d^3/R_i)Z_i^2$. Thus, if R_i does not change during an experiment, the membrane resistance R_m (or conductance $G_m = 1/R_m$) at any time t can be compared with that of any reference value R_{m0} (or G_{m0}) as: $G_{m0}/G_m = R_m/R_{m0} = (d/d_0)^3(Z_i/Z_{i0})^2$, where Z_i and d are values measured at time t, compared to the reference values Z_{i0} and d_0 (normally taken here as those at pH 7.0). In experiments here, R_i and diameter ordinarily do not change over many hours in a viable axon. Some water uptake by the axon typically occurs with the saline used here. If the axon is initially under some tension, axon turgor increases and membrane resistance will typically double in 10-30 min and then stabilize with minimal change in axon diameter. If the axon is kept flaccid, as most often was done here, the membrane resistance rise was minimal.

To determine cable impedance with sinusoidal waves, the sinusoidal voltage $V(x)$ produced across the axon membrane by the injected current was amplified to around 1 V (for $x = 0$), and multiplied with an in phase constant voltage output V_f (1 V here) from the oscillator (Fig. 1). The multipler output $kV_fV(x)$, (gain = k), is passed through an adjustable low band pass DC amplifier whose output is thus proportional to the peak value of $V(x)$. This allows the determination of λ and the axon cable input impedance, since $Z_i = V(x = 0)/I$. Selection of the upper frequency limit for the band pass amplifier adjusts the response time for observing membrane resistive changes. This autocorrelation technique reduces much of the error due to noise and membrane potential fluctuations which normally occur during an experiment. The precision and sensitivity of this circuit has been well below 1%.

The difference between axon cable properties at 15 Hz and DC can be shown to be minimal. From cable theory (Tasaki and Hagiwara, 1957; Falk and Fatt, 1964; Schneider, 1970), for $R_m = 10^3$ Ω cm^2, $C_m = 10^{-6}$ F/cm^2, $R_i = 40$ Ω cm, $d = 100$ μm, the ratio: $Z(f = 15\text{ Hz})/Z(f = 0) = 0.998$ for $x = 0$, and 0.995 for $x = 3\lambda$. The corresponding phase shifts between injected current and recorded membrane potential are 2.7° ($x = 0$), and 6.7° ($x = 3\lambda$). The corresponding error $[Z(f = 15\text{ Hz}) - Z(f = 0)]/Z(f = 0)$ in the impedance-measuring cirtuit (Fig. 1) due to amplitude and phase differences to the two inputs of the multiplier can be calculated to be 0.3% ($x = 0$), and 1.2% ($x = 3\lambda$). Since the useful measurements are ordinarily

obtained from $x = 0$ to 1λ, the errors here are minimal and the axon cable properties at 15 Hz may be considered as that at DC.

Solutions

The saline utilized contained (mM): NaCl 205, KCl 5.4, $CaCl_2$ 13.5, $MgCl_2$ 2.6. Either no buffer, or 5 or 10 mM of Tris or Tris-maleate was used. pH was adjusted by adding HCl or NaOH. Changes in ion concentrations were done by one-to-one substitution to maintain constant osmotic strength and ionic activities of other ions (Strickholm and Wallin, 1967). Sodium was exchanged with choline, potassium by sodium, and chloride by either isethionate, glucuronate, or propionate. Below pH 5, only isethionate substitution appeared satisfactory. Ion concentration changes were ordinarily done so that each examined ion was altered in the ratio of 5.4:10 or the inverse, although other ratios were examined. Temperatures were around 20°C.

Ionic Permeability and Conductance

Membrane ionic permeabilities and conductances are calculated here using the fixed charge theory of Teorell (1953) and compared with the formulation of the parallel branched equivalent circuit (Schwartz, 1971; Finkelstein and Mauro, 1963; Hodgkin and Huxley, 1952).

The technique of measuring the ionic dependency of the membrane potential or transference number T_j has been previously described (Strickholm and Wallin, 1967; Hodgkin and Horowicz, 1959). In this method, a sudden step change in one of the permeable ions is made by replacement with an equivalently charged but much less permeable ion (to preserve ionic strength and osmolarity), and the resulting change in membrane potential ΔV_m observed. The specific ionic dependency T_j of the membrane potential on a jth ion is defined as: $T_j = \partial V_m / \partial E_j \simeq \Delta V_m / \Delta E_j$, where ΔE_j is the change in the Nernst potential for the jth ion. If intracellular concentrations do not change, ΔE_j may be written as $(RT/zF) \ln (C_{jf}/C_{j0})$, where C_{jf} and C_{j0} are the final and initial external ion concentrations for the jth ion, z the ion charge, and $(RT/F) = 0.025$ V at 20°C. The operational measurement T_j represents in the parallel branched circuit the partial conductance (g_j/G_m) and the actual ionic transference number (Hodgkin and Horowicz, 1959). In the fixed charge theory of Teorell, T_j does not have these specific interpretations. Thus, although the operational definition of T_j is valid whatever the membrane model examined, its interpretation will vary depending upon the membrane model.

In the experiments here, the following were measured as a function of pH: the membrane potential, V_m; the specific ionic potential dependencies, T_K, T_{Cl}, and T_{Na}; and axon input impedance, Z_i. By utilizing the axon cable measurements λ, Z_i, and diameter d, the membrane resistance R_m or conductance G_m was obtained. From this data as described below, specific ionic permeabilities P_j (fixed charge model) or conductances g_j (parallel-branched circuit) were calculated as a function of pH.

The parallel-branched circuit model (Hodgkin and Huxley, 1952) gives:

$$I_j = g_j(V_m - E_j); \quad \Sigma I_j = 0; \quad \Sigma g_j = G_m; \quad g_j = T_j G_m;$$
$$V_m = \Sigma T_j E_j; \quad \Sigma T_j = 1, \tag{1}$$

where I_j is the membrane current, E_j the Nernst potential, and g_j the specific ionic conductance for the jth ion. Summation is over the j ions.

In this model, the determination of the specific ionic conductance g_j thus requires only the measurement of T_j and G_m, and the potential dependencies become hidden in g_j.

The fixed charge theory of Teorell (1953) considers the membrane as a homogenous domain with ionic permeabilities determined by membrane fixed charge density and specific membrane ionic mobilities. The membrane fixed charge density appears in the ionic flux equations of Teorell in the Donnan ion distribution ratio r (concentration in the membrane with respect to solution), where

$$r = [1 + (w\overline{X}/2a)^2]^{1/2} - w\overline{X}/2a. \tag{2}$$

w and $\overline{X}$ represent the charge and membrane fixed charge concentration, and a is the bulk external concentration (Teorell, 1953, p. 320). From Teorell (1953, Eq. 28), the membrane potential (external side referenced here as zero) for *equal* external and internal concentrations may be written as:

$$\exp(-FV_m/RT) = \xi = (rU_i + V_0/r)/(rU_0 + V_i/r), \tag{3}$$

where

$$U_i = \Sigma u_j C_{ji}; \qquad U_0 = \Sigma u_j C_{j0}; \qquad V_i = \Sigma u_j A_{ji}; \qquad V_0 = \Sigma u_j A_{j0}, \tag{4}$$

and u_j is the ion mobility, C_{ji} and C_{j0} the inside and outside cation concentration; A_{ji} and A_{j0} the inside and outside anion concentration for the jth ion. Summation is over the j ions.

These expressions (Eq. 4) refer to all ion species present. Ordinarily, most ion species other than K, Cl, and Na have membrane mobility-concentration products (u_jC_j or u_jA_j) so small that their contribution can be neglected in Eq. 4. Their omission does not affect the final expressions for membrane ion permeabilities (Eq. 10–11). Eq. 3 has the advantage of being more general, in that it was derived by Teorell without constraints on the form of the membrane potential gradient, although Finkelstein and Mauro (1963, Appendix I) showed that equal concentrations on both sides of the membrane implies a constant field. For zero membrane charge ($w\overline{X} = 0, r = 1$), Eq. 3 is identical to the constant field equation.

If intracellular concentrations are kept constant, and an extracellular ion is altered, we have by definition: (for a cation):

$$T_j = \partial V_m/\partial E_j = (FC_{j0}/RT)(\partial V_m/\partial C_{j0}) = ru_jC_{j0}/(rU_0 + V_i/r), \tag{5}$$

and (for an anion):

$$T_j = \partial V_m/\partial E_j = (FA_{j0}/RT)(\partial V_m/\partial A_{j0}) = (u_jA_{j0}/r)/(rU_i + V_0/r). \tag{6}$$

The diffusion coefficient $D_j(\mathrm{cm}^2/\mathrm{s}) = u_jRT$ and the membrane permeability is:

$$P_j' = D_j/\delta = u_jRT/\delta\,(\mathrm{cm/s}), \tag{7}$$

where δ is the membrane thickness.

$$\text{Define: (for a cation): } P_j = rP_j'\text{; (for an anion): } P_j = P_j'/r. \tag{8}$$

The membrane conductance (per unit area) $G_m = \partial I/\partial V_m$ at zero membrane current, or at resting membrane potential, is given by Teorell (1953, Eq. 34) and is recast here as:

$$G_m(I = 0) = (F^2/\delta)(rU_0 + V_i/r)(\xi \ln \xi)/(\xi - 1) \tag{9}$$

This equation is similar to that obtained by Hodgkin and Katz (1949) except for the term r due to membrane fixed charges. Utilizing Eqs. 3 and 5–9, we have:

$$\text{(for a cation):}\quad P_j = rP'_j = (RT/F^2)(1/C_{j0})[(\xi - 1)/\xi \ln \xi](T_j G_m), \tag{10}$$

$$\text{(for an anion):}\quad P_j = P'_j/r = (RT/F^2)(1/A_{j0})[(\xi - 1)/\ln \xi](T_j G_m). \tag{11}$$

For the major permeable ions, K, Cl, and Na, this gives:

$$P_K = rP'_K = (RT/F^2)(1/K_0)[(\xi - 1)/\xi \ln \xi](g_K), \tag{12}$$

where $g_K = T_K G_m$,

$$P_{Na} = rP'_{Na} = (RT/F^2)(1/Na_0)[(\xi - 1)/\xi \ln \xi](g_{Na}), \tag{13}$$

where $g_{Na} = T_{Na} G_m$,

$$P_{Cl} = P'_{Cl}/r = (RT/F^2)(1/Cl_0)[(\xi - 1)/\ln \xi](g_{Cl}), \tag{14}$$

where $g_{Cl} = T_{Cl} G_m$.

Eqs. 10 and 11 thus allow the specific ionic permeabilities to be determined from measurements of V_m, T_j, and the resting membrane conductance G_m. Eqs. 10 and 11 are seen to be related to conductance (Eq. 1) by multiplication of g_j by a constant B_j dependent on concentration and a potential-dependent term $f(V_m)$, as:

$$P_j = B_j f(V_m) g_j, \qquad \text{where:} \qquad g_j = T_j G_m \tag{15}$$

Thus for a constant membrane potential, the specific permeability P_j and conductance g_j differ by only a constant multiplying term.

Eqs. 12 and 13 provide ionic permeability ratios as:

$$P_{Cl}/P_K = (P'_{Cl}/r)/rP'_K = T_{Cl} K_0 \xi / T_K Cl_0, \tag{16}$$

$$P_{Cl}/P_{Na} = (P'_{Cl}/r)/rP'_{Na} = T_{Cl} Na_0 \xi / T_{Na} Cl_0, \tag{17}$$

$$P_{Na}/P_K = P'_{Na}/P'_K = T_{Na} K_0 / T_K Na_0. \tag{18}$$

Eqs. 3 through 8 give:

$$\Sigma T_{cj} \xi_{cj} = (1 - \Sigma T_{Aj})\xi \tag{19}$$

$$\xi \Sigma T_{Aj} \xi_{Aj} = (1 - \Sigma T_{cj}), \tag{20}$$

where T_{cj} and T_{Aj} are the transference numbers for the jth cation and anion respectively, $\xi_{cj} = C_{ji}/C_{j0}$, and $\xi_{Aj} = A_{ji}/A_{j0}$.

If the only major permeable ions are K, Na, and Cl, Eqs. 19 and 20 give:

$$T_K \xi_K + T_{Na} \xi_{Na} = (1 - T_{Cl})\xi,$$

where:

$$\xi_K = K_i/K_0, \text{ and } \xi_{Na} = Na_i/Na_0, \tag{21}$$

$$V_m = E_{Cl} - (RT/F) \ln [(1 - T_K - T_{Na})/T_{Cl}],$$

where:

$$E_{Cl} = -(RT/F) \ln (Cl_0/Cl_i). \tag{22}$$

Eq. 21 provides a formulation of the membrane potential $V_m = -(RT/F) \ln \xi$ in terms of sodium and potassium concentration ratios and the ionic potential dependencies T_j. If the con-

tribution of $T_{Na}\xi_{Na}$ is negligible, it may be used to estimate intracellular potassium. Eq. 22 allows intracellular chloride activity to be determined from the membrane potential and the T_j's.

RESULTS

All the data described here, unless otherwise indicated, are plotted as starting from pH 7.0 with pH changes going either acid or basic in steps of 0.2 pH units. Consequently, a small discontinuity in slope is ordinarily seen going through pH 7.0. This method for plotting the data was chosen to minimize shifts in data points due to hysteresis effects, which on a return from a pH change can shift data points up to one pH unit (Fig. 6). Fig. 3 shows the steady state membrane potential as a function of pH for a typical axon. An action potential was obtainable over the entire pH range studied, from below pH 4 to above pH 11. Good reversibility of membrane potential was obtainable between pH 5 and 10. Below pH 5, a slow depolarization continuously occurs, and below around pH 3.7–3.8, a rapid (ca. 1 mV/s) irreversible potential and membrane resistance loss begins, which is not reversed by return to neutral pH. Failure in alkaline pH has always resulted from calcium precipitation in the saline, which typically has been around pH 10.5 in these experiments. By utilizing freshly distilled CO_2-free water, the highest pH obtained here before axon failure has been pH 11.4. With calcium precipitation in alkaline pH, irreversible loss of membrane potential and resistance occurred, and was not reversed by return to neutral pH. The data in this paper consist of measurements from several hundred axons having average membrane potentials around that of Fig. 3.

Membrane Resistance and Conductance

Fig. 4 shows the relative dependence of the resistance (R_m/R_{m0}) and conductance (G_m/G_{m0}) ratios on pH, where R_{m0} and G_{m0} are the reference membrane resistance and conductance at pH 7.0 and the average membrane potential of 85.9 mV, and R_m and

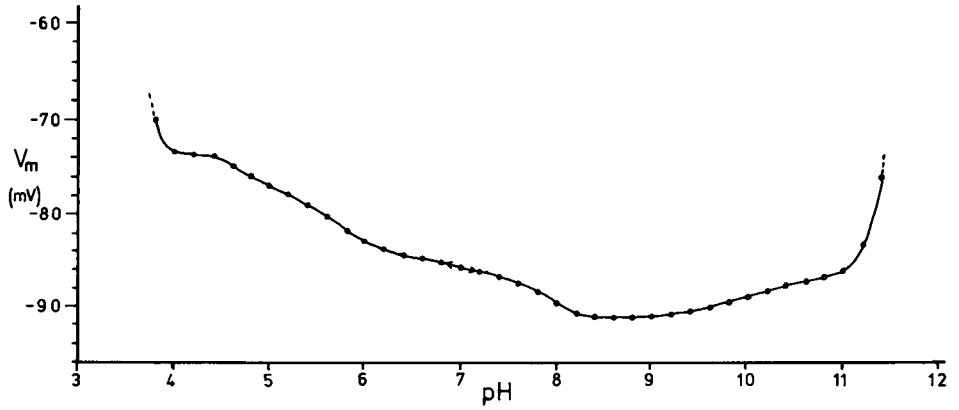

FIGURE 3 The dependency of steady-state membrane potential on pH.

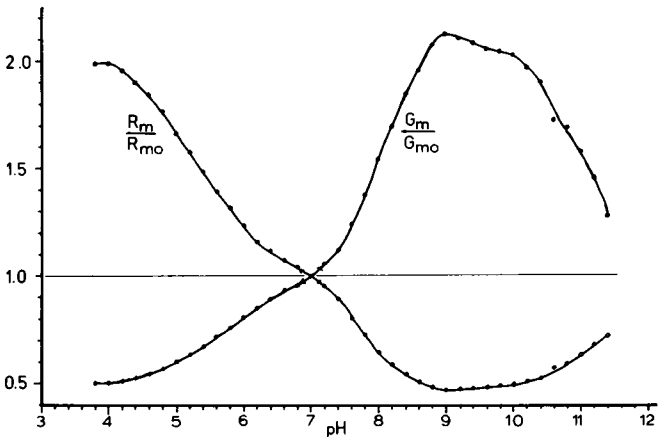

FIGURE 4 The dependency of relative membrane conductance or resistance on pH.

G_m are the membrane resistance and conductance at the pH indicated. In these experiments, R_{m0} = 603 ± 344 (SD) (n = 109) Ω cm^2 and R_i = 37 ± 15 (SD) Ω cm. The data of Fig. 4 are for the membrane potential of Fig. 3. The standard deviation for each datum point of R_m/R_{m0} ranges from 0.007 (n = 48) around neutral pH, to 0.36 (n = 16) at pH 5 and 10.0.

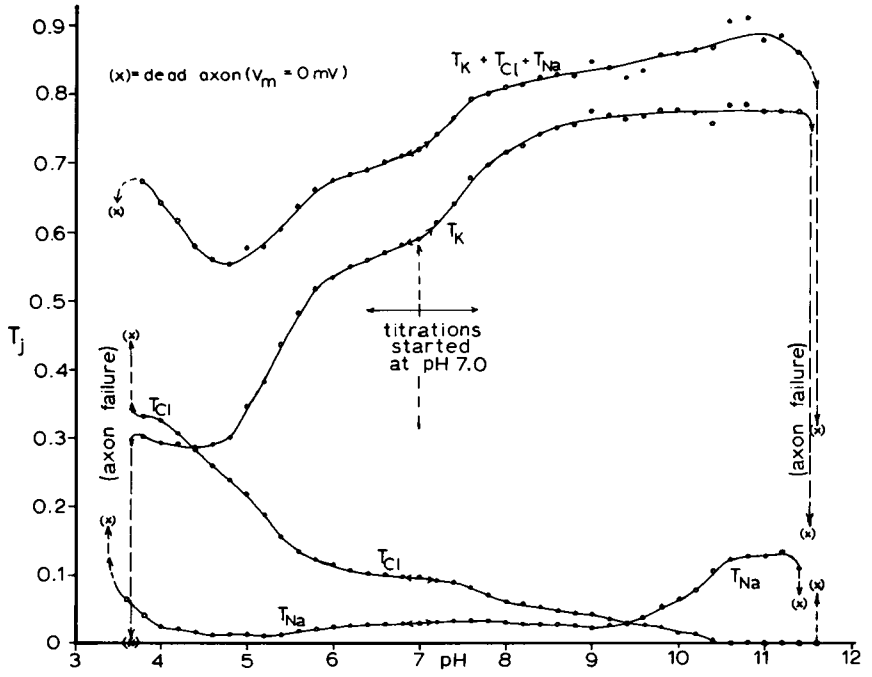

FIGURE 5 The specific ionic dependency of membrane potential on external ions: (T_K) potassium, (T_{Na}) sodium, and (T_{Cl}) chloride. (x) is for dead axon, V_m = 0.

Ionic Dependency of the Membrane Potential (T_j)

Fig. 5 shows the dependency of T_j on pH. The data points were obtained from axons throughout the year. No obvious seasonal variations appeared except around molting time, when the saline utilized could not sustain the axon membrane potential and resistance. Average standard deviations for T_K, T_{Cl}, and T_{Na} were: 0.11, 0.069, and 0.019, respectively ($\bar{n}$ = 19). Transitions are observed in T_j at several pH regions, the steepness of which has varied from axon to axon. The pH regions of these transitions have not, however, been variable. Below pH 4.0, all the T_j's increase before loss of membrane potential. In the extreme alkaline region, T_K becomes asymptotic and T_{Cl} becomes zero, while T_{Na} continuously increases until membrane failure occurs. The datum points around pH 11.5 and 3.6 enclosed by parentheses indicate typical values in the failed axon when the membrane potential has fallen to zero.

Hysteresis and Variability of Membrane Properties

In general, on returning from an acid or alkaline pH change, the membrane parameters (G_m, T_j, V_m) show hysteresis, the magnitude of which varies, and depends on which ionic groups have been titrated and how much. Hysteresis, similar to that observed here, is commonly seen when titrating large protein molecules and indicates irreversibility. Fig. 6 shows a typical hysteresis loop of resistance vs. pH around neutrality. A pH excursion, as in Fig. 6, has in some experiments shifted data points an entire pH unit. For this reason, the data plotted here are from dissections initiated ordinarily in pH 7.0 and titrated from pH 7.0 in either an acid or basic direction. Dissections done in extreme acid or alkaline pH and titrated in the opposite pH direction show data similar to that shown here except for displacement of the data points. The magnitude of the conductance changes with pH varies from axon to axon, but the transition regions remain at the same pH, provided the dissection saline and titration origin are around neutral pH. Around pH 8, the slope and magnitude of the conduc-

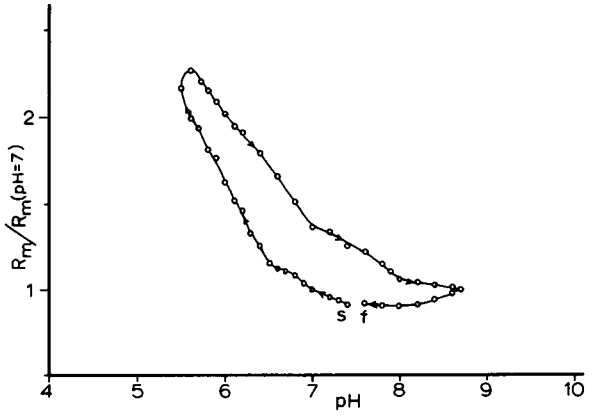

FIGURE 6 Hysteresis of membrane resistance with pH titration. Arrows indicate direction of titration. s = start, f = finish.

tance change with pH is very variable and a minimal change here does not preclude excitability. Similarly, the conductance change over the imidazole region, pH 7–5, is quite variable. However, a large conductance change here typically coincides with an axon having a large action potential.

Ionic Permeability and Conductance

Fig. 7 shows the specific ionic conductances $g_j = T_j G_m$ based on the data compiled in Figs. 4 and 5, and G_{m0} (pH = 7.0) = 1/603 = 1.66×10^{-3} Ω^{-1} cm^{-2}. Fig. 8 depicts the specific ionic permeabilities calculated from Eqs. 12–14, and the data from Figs. 3–5. The specific ionic permeabilities at pH 7.0 are: $P_K = 1.33 \times 10^{-5}$, $P_{Cl} = 1.49 \times 10^{-6}$, and $P_{Na} = 1.92 \times 10^{-8}$ cm/s. The value found here for P_K is consistent with that found for squid nerve (1.7×10^{-4} cm/s, Stein, 1967; 1.8×10^{-6} cm/s, Hodgkin and Katz, 1949, p. 75). The ratio at pH 7.0 of $P_K : P_{Cl} : P_{Na}$ is 693:78:1. In comparison, the conductance ratio at pH 7.0 for $g_K : g_{Cl} : g_{Na}$ is 18.3:3.04:1. Fig. 9 shows the ratio of P_{Cl}/P_K, P_{Cl}/P_{Na}, and P_{Na}/P_K *vs.* pH calculated from Eqs. 16–18. Observed is an approximate constancy of P_{Na}/P_K from pH 5 through 9, a region where a major permeability increase occurs for both these ions. This suggests that sodium and potassium have common controls and possibly share common permeation pathways over this pH region. Also indicated in Fig. 8 are the approximate pK regions reported for ionizable groups of protein and membrane lipid (Tanford, 1962; Steinhardt and Beychok, 1964; Seimiya and Ohki, 1973).

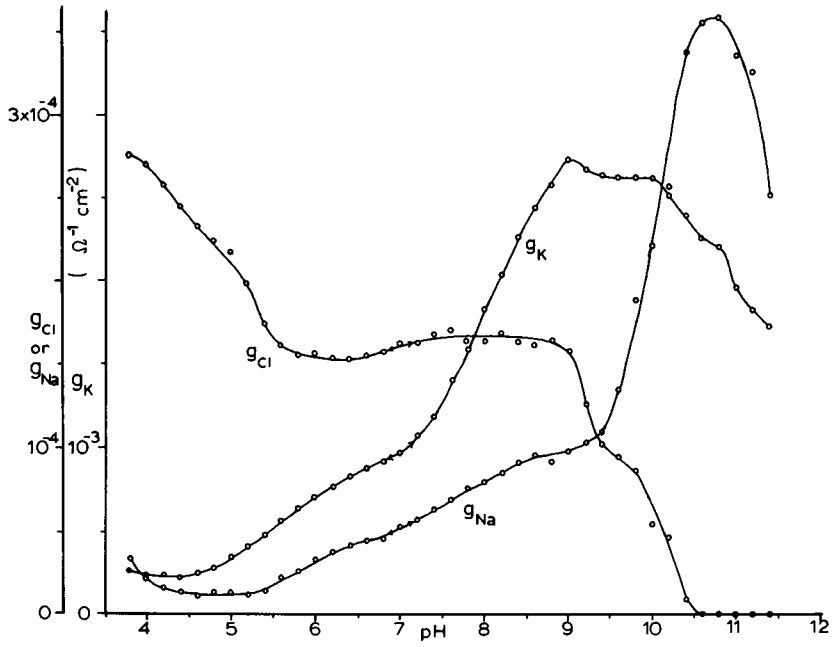

FIGURE 7 Specific ionic conductances, dependency on pH.

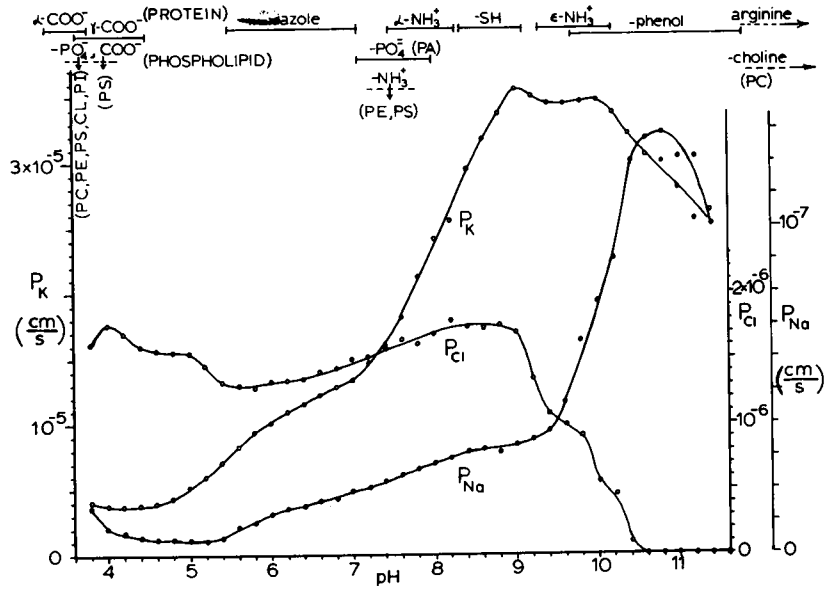

FIGURE 8 Specific ionic permeabilities, dependency on pH.

Role of Surface Membrane Groups in Action Potential and Ionic Permeability

Photooxidation of the axon surface with methylene blue or rose bengal produces an immediate loss of action potential, followed by a rapid loss of membrane potential (Clark and Strickholm, 1971). Photooxidation by rose bengal is considered somewhat selective for histidine (Means and Feeney, 1971, p. 166). The loss of the action potential observed here by chemical change of histidine is consistent with the observation

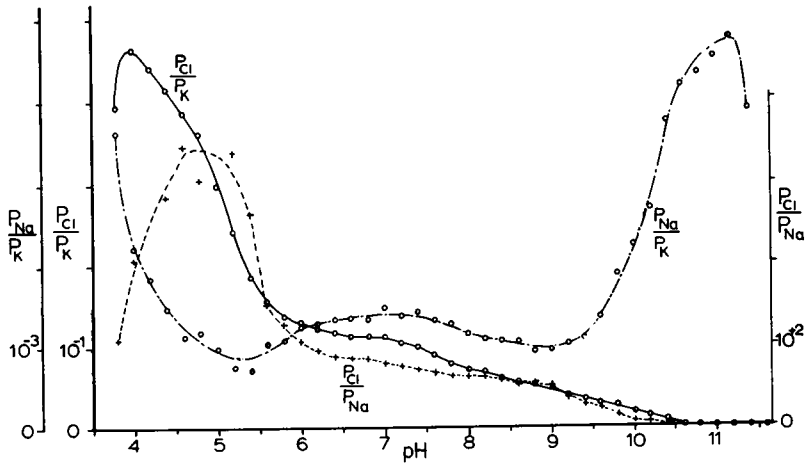

FIGURE 9 Relative ionic permeabilities.

that a step reduction in osmotic pressure (osmotic shock) can eliminate the action potential without significant loss of resting potential. Here, the cooperative conformational change in the cell surface over the imidazole region with pH in the depolarized membrane (Clark and Strickholm, 1971), is no longer observed after the loss of the action potential by osmotic shock (author's unpublished data).

The protein group reagents di- and fluorodinitrobenzene (FFDNB, FDNB) also eliminate the action potential (ca. 10 min at 10^{-6} M FDNB) without reducing the membrane potential sufficient for sodium inactivation (Strickholm et al., 1970, Strickholm and Shrager, 1970). FFDNB is an order faster than FDNB in its effects here. These reagents, which produce neutrally charged products, react primarily with amino groups and also, but slower with imidazole, sulfhydryl, and phenol groups. They additionally react with phosphatidyl serine and phosphatidyl ethanolamine (Gordesky et al., 1975). Before the loss of the action potential, FFDNB and FDNB reduce T_{Cl} to near zero.

The reagent *p*-chloromercuribenzoate (PCMB), which appears specific for sulfhydryl groups, gradually eliminates the action potential with minimal change in resting potential. PCMB attaches a negative charge (phenylformic acid) to the sulfhydryl with a pK of 4.2. The typical action of PCMB is twofold, an initial membrane hyperpolarization of several millivolts (maximum V_m change in 2–4 min at 10^{-5} M PCMB), which coincides with chloride permeability loss to near zero, then followed by a slow depolarization of several millivolts, which coincides with a gradual loss of the action potential. For 10^{-5} M PCMB, typical action potential failure requires 6–10 min. A possible interpretation here is that the initial reaction of PCMB is with an exposed sulfhydryl group that reduces Cl permeability by converting to a negative charge (benzoate) or by a conformational effect but with little effect on the action potential. This is followed by a slower reaction of PCMB with a more deeply buried sulfhydryl or other groups which could affect a membrane protein conformation essential for excitation.

The differential action of cyanate (KNCO) at pH 7 and 8 (Means and Feeney, 1971) was utilized to determine the role of α, or terminal, and ϵ-amino groups to ionic permeability and the action potential. At pH 7.0 (KNCO = 1 mM), where cyanate reacts nearly 100 times more rapidly with α or terminal amino groups than ϵ-amino groups, chloride permeability was reduced slowly, with T_{Cl} reduced by 10% in 10 min. However, at pH 8, where ϵ-amino groups are more reactive, the same KNCO concentrations would reduce T_{Cl} to near zero in comparable time. With cyanate removal at pH 8, some recovery of T_{Cl} occurs. At this KNCO concentration (1 mM), ordinarily no loss of action potential occurred. At higher cyanate concentrations (0.2 M NaNCO), a rapid depolarization and action potential loss occurs, reversible only for brief (ca. 10 s) NaNCO exposure. Cyanate produces only uncharged stable products with amino groups but it also reacts reversibly, but more slowly with imidazole, sulfhydryl, and carboxyl groups. These reactive products which reverse and disappear with cyanate removal could explain the partial recovery of T_{Cl} and reversibility of the action potential loss. If FFDNB (10^{-4} M) is added after 10 min of KNCO (1 mM), treatment and removal at pH 7, T_{Cl} is reduced further, to near zero. After similar

treatment with KCNO at pH 8, where T_{Cl} is reduced to near zero, an addition of FFDNB has minimal further effect on T_{Cl}. Here, upon removal of cyanate and FFDNB, the partial recovery of T_{Cl} seen when cyanate is removed at pH 8 is no longer observed and T_{Cl} remains near zero. Since FFDNB reacts irreversibly with amino, sulfhydryl, tyrosine, and imidazole groups, the above results suggest that although ϵ-amino groups contribute to a major portion of chloride permeability activation from pH 10.6 to 8, the sulfhydryl and tyrosine groups are also partially involved (see Fig. 8).

The effect on cation permeability of the above reagents (PCMB, FDNB, NCO) around neutral pH has ordinarily been minimal. In general, when T_{Cl} falls, both T_K and T_{NA} increase, as expected from Eqs. 1, 19, or 20. However, total membrane conductance G_m typically decreases after KNCO and PCMB treatment. Thus the calculated specific membrane conductances g_K and g_{Na} (or P_K and P_{Na}) appear here minimally affected by KNCO or PCMB. With the reagents FDNB and FFDNB, which react irreversibly with the imidazole group in addition to amino, sulfhydryl, and phenol groups, g_K appears minimally affected at pH 7 while g_{Na} increases by a factor of 2.7. The dependency of ion permeability on pH has not been delineated after membrane treatment with the above reagents.

DISCUSSION

The results shown here (Figs. 7–9) support the fixed-charge concepts of Teorell (1953) that membrane charges regulate ion permeability. Going acid from pH 11, where P_{Cl} is zero, the protonation of tyrosine, ϵ-amino, and sulfhydryl groups from pH 10.6 to 7.5 are primarily responsible for chloride permeation. For cation permeation, the ionization of carboxyl and phosphate (ca. pH 4), of imidazole from pH 5 to 7, and other groups from pH 7 to 9 appears largely responsible. This is consistent with Eq. 2, where the Donnan ratio r, which depends on membrane fixed charge density $w\bar{X}$, controls ion permeability (Eqs. 10 and 11) as $P_{Cl} = (u_{Cl}RT/\delta)/r$, and $P_K = (u_K RT/\delta)r$. Thus with a highly positive membrane, as could occur in acid pH, r goes to zero and P_{Cl} would increase and P_K decrease. Conversely, with a highly negative membrane, as in alkaline pH, r becomes large and P_{Cl} should go toward zero while P_K should increase. These results are observed here. In addition, the introduction of negative charges (PCMB) suppresses chloride permeability. However, in extreme acid and alkaline pH (ca. pH 4 and 11), cation permeability opposite that expected is observed. Other factors such as membrane conformation could be involved here, although in the extremes of pH, membrane failure begins and could account for the deviations from expected fixed-charge membrane permeability.

Other observations supporting membrane charge control of ion permeability have been found for crustacean muscle (DeMollo and Hutter, 1966; Rueben et al., 1962; Hagiwara et al., 1968), *Aplysia* neurons (Brown et al., 1970), and nerve (Hille et al., 1975; Lakshminarayanaiah and Murayama, 1975; and Mozhayeva and Naumov, 1972). In contrast, frog muscle seemingly shows the opposite behavior, where increased membrane protonation decreases chloride conductance and increases that of

potassium (Hutter and Warner, 1967; Mainwood and Lee, 1968; McCrea and Strickholm, 1973). This contrasting behavior of frog muscle to nerve ion permeability with pH supports the view that although membrane fixed charges have a role in ion permeation, the conformational state of the surface membrane protein-lipid also has a significant role (Clark and Strickholm, 1971) as may other factors.

Action potentials were ordinarily observed over the entire pH range studied here. This suggests that the pH effects observed here result primarily from ionizations of the axon external surface, since the action potential in squid axon fails if intracellular pH falls below pH 6.2 and repetitive firing occurs for intracellular pH above 8 or 9.[1] Previous studies on crayfish axons and extracellular pH similarly support the view that intracellular pH is minimally affected with the bicarbonate-free buffers used here (Strickholm et al., 1969). On occasion, a sudden action potential loss would occur around pH 5 (more often with 5–10 mM Tris-maleate buffer, rarely with no buffer) with no loss of membrane potential, suggesting a change in intracellular pH. These data were not used here.

There is evidence that many membrane proteins have preferred orientations with the terminal amino group external and the terminal carboxyl group in the cell interior (Marchesi et al., 1973). Experiments on this crayfish axon suggest this may be true here also. Carboxypeptidase applied externally has minimal effect on ion permeabilities, while leucine amino peptidase gradually reduces chloride ion permeability (Strickholm and Clark, 1971). Both these enzymes applied externally had no effect on the action potential. In contrast, both carboxy and amino peptidases applied internally suppress excitability of squid axons (Tasaki, 1968). The results here and those on squid axons with proteases suggest that membrane protein has carboxyl groups oriented to the interior of the axon. Thus the terminal amino groups appear to have a complex orientation with a group regulating chloride permeability on the surface membrane exterior and a group involved in excitation more accessible from the axoplasm.

Axon failure in extreme alkaline pH has always been simultaneous with calcium precipitation in the saline solution. Whether ionization changes of arginine or choline in the extreme alkaline region can produce axon failure has not yet been determined. The authors (unpublished data) have found that low external calcium (ca. 0.5 mM) results here in an irreversible loss of membrane potential, excitability, and a several-fold membrane conductance increase. In studies on phospholipid liquid crystals, Papahadjopoulus and Bangham (1966) found that a structural modification occurs in the phosphatidylserine-calcium complex at calcium concentrations around 0.8–1.0 mM. Below this calcium concentration, dissociation of the phospholipid-calcium complex occurs. In surface film monolayers and in the presence of calcium (1 mM and above), phosphatidylcholine (PC), phosphatidylserine (PS), and phosphatidylinositol (PI) show no apparent surface potential change from pH 4 to 11. In contrast, changes in

[1] Fishman, H. M. 1970. Personal communication on unpublished data from voltage-clamped perfused squid axons.

surface film potential are seen in phosphatidylethanolamine (PE) from pH 7 to 11, and in phosphatidic acid (PA) from pH 6 to 8. In the acid region (ca. below pH 4), all the phospholipid phosphates become protonated and show surface potential changes (Papahadjopoulus, 1968). At these low pH's, where axon failure occurs, calcium appears to be displaced from phospholipid phosphate and carboxyl (Seimiya and Ohki, 1973). Thus the role of calcium in binding and shielding specific ionic groups appears central in some of the membrane permeability-controlling groups. This view is supported by D-Arrigo (1975), where screening of surface membrane phosphate by divalent cations has a role in excitation and passive ion permeability.

Potassium ion permeability (Figs. 7 and 8) appears already to be partially activated at Ph 4. However, its primary control appears to be partly from pH 5 to 7 by ionization of imidazole, and largely from pH 7 to 9 by either the phosphate of PA or an amino group of protein or phospholipid. For reasons described above, the amino group of PS may not be involved, since in calcium solutions it shows no surface potential change in monolayers with pH until pH 11 (Papahadjopoulos, 1968). PE, however, does show surface potential changes from pH 7 to 9. However, KNCO, which alters amino groups, affects P_K minimally. In addition, the results with leucine amino peptidase show minimal changes in potassium permeability at pH 7. This suggests that amino groups are not involved here and that PA is the component that regulates potassium permeability over pH 7–9. In Fig. 8, the ionization of sulfhydryls may affect potassium permeability. However, the use of mercurials, which affect SH groups, minimally affect P_K. In the alkaline region, pH 10 and above, both potassium and chloride permeabilities decrease with the ionization of what may be phenolic groups. This suggests that in this alkaline region, tyrosine may exert more a conformational type control than a fixed charge control on permeability.

Sodium permeability parallels that of potassium from around pH 5 to 9 (Fig. 9), suggesting that common fixed charged groups regulate both these cations and that they may share common permeable pathways. However, in the far alkaline and acidic regions, P_{Na}/P_K increases, suggesting that if a common channel were permeable to both ions, the channel selectivity changes here with membrane fixed charge changes. This change in sodium to potassium selectivity with charge could be similar to that found with charged ionophores in lipid bilayers. That FDNB but not KNCO affects sodium permeability suggests that phenolic groups are involved above pH 9.

The opening of chloride permeability appears from Fig. 8 to result from protonated states of phenolic (tyrosine), ϵ-amino, and sulfhydryl groups. At normal physiological pH (7–7.5), all these groups are protonated and chloride is near maximum permeability. The results with KCNO at pH 8, which replaces amino groups with a neutral amide and considerably reduced P_{Cl}, suggests that ϵ-amino groups (lysine) are the primary regulatory groups for chloride permeability. The further reduction of P_{Cl} to essentially zero by FDNB suggests a further contribution to chloride permeability by tyrosine or sulfhydryl. To what extent fixed charge or conformational control is involved is uncertain. In Fig. 8, it is seen that from pH 9 to 5.7, P_{Cl} gradually decreases.

In part, this results from the potential dependency term for P_{Cl} (Eq. 14) decreasing from pH 9 to 5.7 (90.9–81.5 mV, Fig. 3), more than an observed increase in g_{Cl} with depolarization (authors' unpublished results). Thus at constant membrane potential, this decrease in P_{Cl} from pH 9 to 5.7 would not occur. From pH 5.7 to 4, the small chloride permeability increase appears to result from protonation of carboxyl or phosphate groups. Since protein carboxyl groups are most likely oriented toward the axon interior, chloride permeability increase probably results here from protonation of phospholipid phosphate or the carboxyl of PS.

In the parallel-branched membrane model (Eq. 1; Hodgkin and Huxley, 1952; Hodgkin and Horowicz, 1959; Schwartz, 1971), the specific ionic conductances are derived as resulting from separate specific permeable pathways for K, Cl, and Na. In this model $\Sigma T_j = 1$. Fig. 5 shows that the sum $T_K + T_{Na} + T_{Cl}$ is always less than 1 and only approaches unity in alkaline pH where T_{Cl} goes to zero. In the fixed charge model (Teorell, 1953; Schwartz, 1971; Finkelstein and Mauro, 1963), where permeable ions share a common homogenous domain, the operational measurement of T_j no longer represents a transference number as in the parallel-branched model. In addition, ΣT_j does not ordinarily equal unity in the fixed charge model except when T_{Cl} equals zero or when chloride ion is in electrochemical equilibrium (Eqs. 20, 22 here, and Strickholm and Wallin, 1967). Since no other major ions are present to contribute to membrane permeability, a measurement here that ΣT_j does not equal unity suggests that Teorell's fixed charge model is more applicable than the parallel-branched model. This appears more the case in acid pH where chloride and potassium permeability become comparable (Fig. 9). However, in alkaline pH, T_{Cl} becomes zero and T_K and T_{Na} approach 0.9 and not unity as expected for both membrane models. The reasons for this are not completely understood but result in part from errors introduced by the first-order method of measuring the T_j's, which neglects here the change in other ion transference numbers when changes in one ion are made. These cross-term corrections have been considered in the approach of Hodgkin and Horowicz (1959) but are not included in the analysis here. This error in the T_j's has been measured here to be around 5%. Thus in alkaline pH, a distinction between the two membrane models is not possible on the basis of the T_j measurements. It must be emphasized that this distinguishing between these two membrane models is for passive ion permeability at zero membrane current and not for that of the excited membrane where membrane currents are not zero.

Eq. 22 defines the membrane potential V_m in terms of the chloride equilibrium potential E_{Cl} and the T_j's. Fig. 10 shows the calculation of E_{Cl} based on the potential data of Fig. 3 and the T_j data of Fig. 6. The results show that Eq. 20 gives an essentially constant E_{Cl} except for alkaline pH. The explanation for the discrepancy in alkaline pH could be that measurement of T_{Cl} near zero is uncertain and ΣT_j does not equal unity when $T_{Cl} = 0$, for reasons discussed above. The results thus support the view that intracellular concentrations change minimally over the pH range examined.

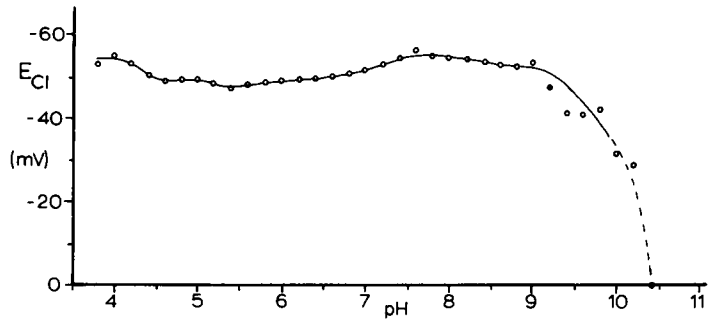

FIGURE 10 Chloride equilibrium potential calculated from V_m and T_j's.

In summary, the data here on ion permeabilities support the theory of Teorell (1953) that membrane fixed charges regulate ion permeabilities in crayfish nerve. It appears that although every possible ionizable membrane group contributes in various degrees to membrane ion permeability, some groups have more specific control in regulating certain ions. Thus passive potassium permeability appears activated partially by phospholipid phosphate and carboxyl (ca. pH 4), secondarily by imidazole groups (pH 5–7), and primarily by ionization, most likely of phosphatidic acid (pH 7–9). Sodium ion permeability appears to be activated like potassium from pH 4 to 9. From pH 9.4 to 11, a threefold increase in P_{Na} occurs, which probably involves tyrosine. Chloride ion permeability seems primarily to be activated by protonation of ϵ-amino groups (pH 10.6–9), in part by tyrosine and sulfhydryl, and further by phospholipid carboxyl or phosphate (pH 5.5–4). In addition, the integrity of imidazole and sulfhydryl groups appears essential for the action potential. The function of these various groups may, however, be the one of maintaining appropriate protein or protein-lipid conformation and not necessarily one of having a specific ion channel control. A central problem that remains here is identifying which of the above membrane-ionizable groups belong to which membrane-incorporated components and to what extent permeability regulation results from conformational control in addition to fixed charge control.

Appreciation is extended to Marjorie Ward, Karen Kruse, and Suman Olivelle, who provided assistance in this work.

This research was supported by grants from the National Institute on Drug Abuse, the National Institutes of Health, and the National Institute on Alcohol Abuse and Alcoholism.

Received for publication 29 November 1976 and in revised form 24 March 1977.

REFERENCES

BROWN, A. M., J. L. WATER, and R. B. SUTTON. 1970. Increased chloride conductance as the proximate cause of hydrogen ion concentration effects in *Aplysia* neurons. *J. Gen. Physiol.* **56**:559–582.

CLARK, H. R., and A. STRICKHOLM. 1971. Evidence for a conformational change in nerve membrane with depolarization. *Nature (Lond.).* **222**:871–872.

D'ARRIGO, J. S. 1975. Axonal surface charges: evidence for phosphate structure. *J. Membr. Biol.* **22**:255–263.

DEMOLLO, W. C., and O. F. HUTTER. 1966. The anion conductance of crustacean muscle. *J. Physiol. (Lond.).* **183**:11*p*.

FALK, G., and P. FATT. 1964. Linear electrical properties of striated muscle fibers observed with intracellular electrodes. *Proc. R. Soc. Lond. B. Biol. Sci.* **160**:69–123.

FINKELSTEIN, A., and A. MAURO. 1963. Equivalent circuits as related to ionic systems. *Biophys. J.* **3**:215–237.

GOLDMAN, D. E. 1943. Potential, impedance, and rectification in membranes. *J. Gen. Physiol.* **27**:37–60.

GORDESKY, S. E., G. V. MARINETTI, and R. LOVE. 1975. The reaction of chemical probes with the erythrocyte membrane. *J. Membr. Biol.* **20**:111–132.

HAGIWARA, S., R. GRUENER, H. HAYASHI, H. SABATA, and A. D. GRINNELL. 1968. Effects of external and internal pH changes on K and Cl conductances in the muscle fiber membrane of a giant barnacle. *J. Gen. Physiol.* **52**:773–792.

HILLE, B., A. M. WOODHULL, and B. I. SHAPIRO. 1975. Negative surface charge near sodium channels of nerve: divalent ions, monovalent ions and pH. *Phil. Trans. R. Soc. Lond. B. Biol. Sci.* **270**:301–318.

HODGKIN, A. L., and P. HOROWICZ. 1959. The influence of potassium and chloride ions on the membrane potential of single muscle fibers. *J. Physiol. (Lond.).* **148**:127–160.

HODGKIN, A. L., and A. F. HUXLEY. 1952. A quantitative description of membrane current and its application to conductance and excitation in nerve. *J. Physiol. (Lond.).* **117**:500–544.

HODGKIN, A. L., and B. KATZ. 1949. The effect of sodium ions on the electrical activity of the giant axon of the squid. *J. Physiol. (Lond.).* **108**:37–77.

HOWLAND. 1966. *In* Applications Manual for Computing Amplifiers. Philbrick Researches, Inc., editors. Nimrod Press, Inc., Boston, Mass. p. 66.

HUTTER, O. F., and A. E. WARNER. 1967. The pH sensitivity of the chloride conductance of frog skeletal muscle. *J. Physiol. (Lond.).* **189**:403–425.

JAIN, M. K. 1972. The Bimolecular Lipid Membrane. Van Nostrand Reinhold Co., New York.

JAIN, M. K., F. P. WHITE, A. STRICKHOLM, E. WILLIAMS, and E. H. CORDES. 1972. Studies concerning the possible reconstitution of an active cation pump across an artificial membrane. *J. Membr. Biol.* **8**:363–388.

LAKSHMINARAYANAIAH, N., and K. MURAYAMA. 1975. Estimation of surface charges in some biological membranes. *J. Membr. Biol.* **23**:279–292.

MAINWOOD, G. W., and S. L. LEE. 1968. The hyperpolarizing effect of hydrogen ions on transmembrane potential in frog skeletal muscle. *Can. J. Physiol. Pharmacol.* **46**:151–157.

MARCHESI, V. T., R. T. JACKSON, J. P. SEGREST, and I. KANHANE. 1973. Molecular features of the major glycoproteins of the human erythrocyte membrane. *Fed. Proc.* **32**:1833–1837.

MCCREA, M. J., and A. STRICKHOLM. 1973. Muscle membrane impedance of the frog sartorius muscle during pH titration. *Biophys. J.* **13**:196*a*. (Abstr.).

MEANS, G. E., and R. E. FEENEY. 1971. Chemical Modification of Proteins. Holden-Day, Inc., San Francisco), Calif.

MOZHAYEVA, G. N., and A. P. NAUMOV. 1972. Effect of surface charge on stationary potassium conductivity of Ranvier node membrane. I. Change of pH of exterior solution. *Biofizika.* **17**:412–420.

MUELLER, P., and D. O. RUDIN. 1968. Resting and action potentials in experimental bimolecular lipid membranes. *J. Theor. Biol.* **18**:222.

PAPAHADJOPOULUS, D. 1968. Surface properties of acidic phospholipids: interaction of monolayers and hydrated liquid crystals with uni- and bi-valent metal ions. *Biochim. Biophys. Acta.* **163**:240–254.

PAPAHADJOPOULUS, D. and A. D. BANGHAM. 1966. Biophysical properties of phospholipids. II. Permeability of phosphatidylserine liquid crystals to univalent ions. *Biochim. Biophys. Acta.* **126**:185–188.

RUEBEN, J. P., L. GIRARDIER, and H. GRUNDFEST. 1962. The chloride permeability of crayfish muscle fibers. *Biol. Bull. (Woods Hole).* **123**:509.

SCHNEIDER, M. F. 1970. Linear electrical properties of the transverse tubules and surface membrane of skeletal muscle fibers. *J. Gen. Physiol.* **56**:640–671.

SCHWARTZ, T. L. 1971. The thermodynamic foundations of membrane physiology. *In* Biophysics and Physiology of Excitable Membranes. W. J. Adelman, editor. Van Nostrand Reinhold Company, New York. 47–95.

SEIMIYA, T., and S. OHKI. 1973. Ionic structure of phospholipid membranes, and binding of calcium ions. *Biochim. Biophys. Acta.* **298**:546–561.

STEIN, W. D. 1967. The Movement of Molecules across Cell Membranes. Academic Press, Inc., New York. 94.

STEINHARDT, J., and S. BEYCHOK. 1964. Interaction of proteins with hydrogen ions and other small ions and molecules. *Proteins.* **2**:139–304.

STRICKHOLM, A. 1968. Reducation of response time for potential in salt bridge reference electrodes for electrophysiology. *Nature (Lond.).* **217**:80–81.

STRICKHOLM, A., and H. R. CLARK. 1971. Alteration of axonal membrane ionic permeabilities by external applied proteases. *Biophys. J.* **11**:55*a*.

STRICKHOLM, A., H. R. CLARK, and P. SHRAGER. 1970. The dependence of membrane ionic permeability and excitation on amino groups. *Biophys. J.* **10**:182*a*. (Abstr.).

STRICKHOLM, A., and P. SHRAGER. 1970. The importance of amino groups in excitation and ionic permeability control. *J. Gen. Physiol.* **55**:145. (Abstr.).

STRICKHOLM, A., and B. G. WALLIN. 1967. Relative ion permeabilities in the crayfish giant axon determined from rapid external ion changes. *J. Gen. Physiol.* **50**:1929–1953.

STRICKHOLM, A., B. G. WALLIN, and P. SHRAGER. 1969. The pH dependency of relative ion permeability in the crayfish giant axon. *Biophys. J.* **9**:873–883.

TANFORD, C. 1962. The interpretation of hydrogen ion titration curves of proteins. *Adv. Protein Chem.* **17**:70–165.

TASAKI, I. 1968. Nerve Excitation, A Macromolecule Approach. Charles C. Thomas, Springfield, Ill.

TASAKI, I., and S. HAGIWARA. 1957. Capacity of muscle fiber membrane. *Am. J. Physiol.* **188**:423–429.

TEORELL, T. 1953. Transport processes and electrical phenomena in ionic membranes. *Prog. Biophys. Chem.* **3**:305–369.

TIEN, H. T. 1974. Bilayer Lipid Membranes. Marcel Dekker, Inc., New York.

WEIDMANN, S. 1952. The electrical constants of Purkinje fibres. *J. Physiol. (Lond.).* **118**:348–360.